

# Vacuum energy density from a self-interacting scalar field in a Lorentz-violation Hořava-Lifshitz model

<sup>1</sup>A. J. D. Farias Junior,<sup>\*</sup> <sup>2</sup>E. R. Bezerra de Mello,<sup>†</sup> and <sup>2</sup>Herondy Mota<sup>‡</sup>

<sup>1</sup>*Instituto Federal de Alagoas,*

*CEP: 57460-000, Piranhas, Alagoas, Brazil and*

<sup>2</sup>*Departamento de Física, Universidade Federal da Paraíba,  
Caixa Postal 5008, João Pessoa, Paraíba, Brazil*

In this paper we consider a massive self-interacting scalar quantum field in a Lorentz-violation scenario based on a Hořava-Lifshitz model. Specifically, we investigate the vacuum energy density and its loop correction, up to first order in the self-interaction coupling constant, and also the topological mass generation. These quantities are also analyzed in the case where the field is massless. The scalar vacuum state is perturbed by the presence of two large parallel plates, placed at a distance  $L$  from each other, due to the imposition of Dirichlet boundary condition on the two plates. To perform this study, the effective potential approach in quantum field theory is applied.

## I. INTRODUCTION

In 1948, H. Casimir predicted the effect that bears his name, the Casimir effect [1]. This effect is one of the most interesting physical phenomenon and it is considered as a direct consequence of quantum vacuum fluctuations of the electromagnetic field. In the standard approach, Casimir considered a quantized electromagnetic field confined in a region between two perfectly conducting parallel neutral plates, placed in vacuum very close to each other. Due to modifications of the vacuum fluctuations imposed by the boundaries, a force of attraction arises between the plates. Although with low accuracy, the first attempt to experimentally confirm the Casimir effect was performed in [2], followed several years later by others high accuracy experiments [3–9]. Besides the electromagnetic field, others fields such as the scalar and fermionic, also presents Casimir-like effects manifesting in the form of a nonzero vacuum energy density. For instance, considering scalar fields, the Casimir effect with the field subjected to Robin boundary conditions is considered in Ref. [10], subjected to a helix boundary condition with temperature corrections in Ref. [11], and in Ref. [12] the Casimir effect is investigated in the classical geometry of two parallel conducting plates, in a noncommutative spacetime within a coherent state approach. A review on the Casimir effect can be found in Ref. [13–15].

Since the Theory of Relativity is the basis for quantum field theory, the standard approach for the investigation of the Casimir effect is assuming that the Lorentz symmetry is preserved. However, high energy scale theories fail to preserve the Lorentz symmetry [16, 17]. In a scenario where the Lorentz symmetry violation is allowed the spacetime becomes anisotropic, modifying the modes of the quantum field and as a consequence, the vacuum energy density is affected. The Lorentz symmetry violation is an interesting topic which has been attracting a great deal of attention, mainly because it is an alternative to investigate new physics beyond the standard model. In Ref. [18] the authors considered a scalar field under helix boundary condition in a scenario with a CPT-even aether-type Lorentz symmetry violation to study vacuum energy density. Thermal corrections to the vacuum energy density in a Lorentz-breaking scalar field theory is considered in Ref. [19]. Considering finite temperature and an external magnetic field, the corrections to the vacuum energy due to the Lorentz violation is investigated in [20]. In Ref. [21] it was considered the Casimir like-effect with Lorentz symmetry violation in a theory with high order derivatives. The Lorentz symmetry violation is also studied in the context of string theory [16], and in low-energy scale in Refs. [17, 22–31]. Considering a quantum gravity scenario, the Horava–Lifshitz formalism, [32], breaks the Lorentz symmetry in a strong manner. Due to different space and time scaling properties in Hořava-Lifshitz framework, the spacetime becomes anisotropic which modifies the quantum vacuum fluctuations and consequently, the vacuum energy density [33].

In the present paper we consider a massive scalar quantum field in a Hořava-Lifshitz (HL) model. Our main objective is to analyze how the strong Lorentz violation affects the vacuum state considering that a real scalar field is confined in the region between two large parallel plates placed perpendicular to the  $z$ -direction, and separated by a short distance  $L$ . We impose that the field satisfies Dirichlet boundary condition on these plates. In addition, it

---

\*Electronic address: [antonio.farias@ifal.edu.br](mailto:antonio.farias@ifal.edu.br)

†Electronic address: [emello@fisica.ufpb.br](mailto:emello@fisica.ufpb.br)

‡Electronic address: [hmota@fisica.ufpb.br](mailto:hmota@fisica.ufpb.br)

is included a self-interaction potential which is represented by a term proportional to the fourth power of the real scalar field, i.e., a  $\varphi^4$  theory. Using the path integral approach to obtain the effective potential [34], we develop the investigation of the vacuum energy density and its loop correction in the Horava-Lifshitz formalism. Furthermore, the topological mass which arises due to the boundary condition and also due to the Lorentz symmetry violation is investigated.

This paper is organized as follows: in Sec. II we review the main aspects of the Hořava-Lifshitz model, including a self-interaction potential, and the path integral formalism that we apply for the investigation we develop here, as well as the generalized zeta function technique to write the path integral in a convenient form. In Sec. III, we impose Dirchlet boundary condition on the quantum field and obtain the generalized zeta function, which allows us to write the one-loop correction and the effective potential. Sec. IV is dedicated to the analysis of the vacuum energy density for the case of both massive and massless fields, which shows a dependence on the boundary conditions obeyed by the fields and also on the Lorentz symmetry violation. In addition, the correction for the vacuum energy density is also considered in this section. Next, in Sec. IV C, we investigate the possibility of a topological mass arising due to the boundary condition, self-interaction potential and the Lorentz violation within the Hořava-Lifshitz formalism. In Sec. IV D we estimate the ratio between the parameter associated with the Lorentz violation and the length separation  $L$  between the plates. Finally in Sec. V we present our conclusions. Throughout this paper we use natural units in which both the Planck constant and the speed of light are set equal to unity,  $\hbar = c = 1$ .

## II. HOŘAVA-LIFSHITZ THEORY AND THE ONE-LOOP CORRECTION

We first consider a massive real scalar quantum field, in a theory where the space and time have different properties by rescaling. This difference provides a spacetime anisotropy and as a consequence the Lorentz symmetry violation. The spacetime anisotropy, makes the theory invariant under the following scale transformation:

$$x \rightarrow bx, \quad t \rightarrow b^\xi t, \quad (1)$$

where  $\xi$  is a critical exponent [32]. In the 4-dimensional Euclidean spacetime and considering a self interacting field  $\varphi$ , we can write the action describing the system as follows [35, 36],

$$S(\varphi) = -\frac{1}{2} \int d^4x \varphi \left[ -\partial_\tau^2 + (-1)^\xi l^{2(\xi-1)} (\partial_x^2 + \partial_y^2 + \partial_z^2)^\xi \right] \varphi - \int d^4x V(\varphi), \quad (2)$$

where

$$V(\varphi) = \frac{1}{2} m^2 \varphi^2 + \frac{\lambda}{4!} \varphi^4, \quad (3)$$

includes the mass and the self-interaction of the field. The parameter  $l$  in the above expression has dimension of length, and has been introduced to make the dimension of the Lagrangian density compatible. Note also that  $m$  is the mass of the field and  $\lambda$  is the coupling constant of the self-interaction.

Using the path integral approach, we construct the effective potential in order to investigate the vacuum energy density and also the topological mass generation within the system considered here. The construction of the effective potential is described in detail in Refs. [34, 37, 38] (see also [39–41]). The expansion of the effective potential in powers of  $\hbar$ , up to order  $\hbar^2$ , can be written as,

$$V_{\text{eff}}(\Phi) = V^{(0)}(\Phi) + V^{(1)}(\Phi) + V^{(2)}(\Phi). \quad (4)$$

In the above expression,  $\Phi$  stands for the fixed background field and it is in fact the field about which we expand the action (2), i.e., we set  $\varphi = \Phi + \phi$ , with  $\phi$  representing the quantum fluctuations. The first term in the r.h.s. of the above equation is the zero order term which describes the classical potential, i.e., the tree-level contribution,

$$V^{(0)}(\Phi) = V(\Phi). \quad (5)$$

If needed, one can include counter terms in  $V(\Phi)$  to account for renormalization of the effective potential.

The second term,  $V^{(1)}(\Phi)$ , is the one-loop correction to the classical potential, which can be written in terms of path integral as [18, 34, 38],

$$V^{(1)}(\Phi) = -\frac{1}{\Omega_4} \ln \int \mathcal{D}\varphi \exp \left[ -\frac{1}{2} \int d^4x \varphi(x) \hat{A}\varphi(x) \right], \quad (6)$$

where  $\Omega_4$  is the 4-dimensional volume of the Euclidean spacetime, which depends on the conditions imposed on the fields. Also, the operator  $\hat{A}$  is defined as

$$\hat{A} = -\partial_\tau^2 + (-1)^\xi l^{2(\xi-1)} (\partial_x^2 + \partial_y^2 + \partial_z^2)^\xi + V''(\Phi). \quad (7)$$

The double prime notation in  $V''(\Phi)$ , stands for the second derivative of  $V(\varphi)$  with respect to the field  $\varphi$  calculated at  $\Phi$ , which is the fixed background field. Then, for the theory we consider,  $V''(\Phi)$  takes the following form

$$V''(\Phi) = m^2 + \frac{\lambda}{2}\Phi^2. \quad (8)$$

The one-loop correction to the effective potential can be written in terms of the generalized zeta function, constructed from the eigenvalues of the operator  $\hat{A}$  [18, 38, 42]. Denoting by  $\Lambda_\sigma$  the eigenvalues, the generalized zeta function is defined as,

$$\zeta(s) = \sum_\sigma \Lambda_\sigma^{-s}, \quad (9)$$

where  $\sigma$  denotes a set of quantum numbers associated with the eigenfunctions of the operator  $\hat{A}$ . The summation symbol denotes a sum or a integration of the quantum numbers, depending on whether they are discrete or continuous. Once we construct the generalized zeta function in Eq. (9), we write the one-loop correction to the effective potential in the following form [38, 41, 42]:

$$V^{(1)}(\Phi) = -\frac{1}{2\Omega_4} [\zeta'(0) + \zeta(0) \ln \nu^2]. \quad (10)$$

The notations  $\zeta(0)$  and  $\zeta'(0)$  stand for the generalized zeta function and its derivative with respect to  $s$ , evaluated at  $s=0$ , respectively. The parameter  $\nu$  has dimension of mass and it is an integration measure on the functional space, which is to be removed via renormalization. Moreover, it is more convenient to calculate the two-loop correction to the effective potential from the two-loop Feynman graph. If we are interested only in the vacuum contribution, the two-loop correction can then be written in the terms of the generalized zeta function [39–41]. We postpone the explicit form of the  $V^{(2)}(\Phi)$  until Section IV B.

### III. DIRICHLET BOUNDARY CONDITION, GENERALIZED ZETA FUNCTION AND THE ONE-LOOP CORRECTION

In this section, we apply the Dirichlet boundary condition on two parallel large plates, separated by a distance  $L$  along the  $z$  direction. Within this configuration, the scalar field  $\varphi$  satisfies the following restriction:

$$\varphi(\tau, x, y, 0) = \varphi(\tau, x, y, L) = 0. \quad (11)$$

The above condition implies that the eigenvalues of the operator  $\hat{A}$  given in Eq. (7) takes the form,

$$\Lambda_\sigma = k_\tau^2 + (-1)^{2\xi} l^{2(\xi-1)} \left[ k_x^2 + k_y^2 + \left( \frac{\pi n}{L} \right)^2 \right]^\xi + V''(\Phi). \quad (12)$$

Note that the momentum in  $z$  has been discretized and  $n$  assumes non-negative integers values, that is,  $n = 1, 2, 3, \dots$ . The set of quantum modes in this case is given by  $\sigma = (k_\tau, k_x, k_y, n)$ , with  $(k_\tau, k_x, k_y)$  being the continuous momenta.

The eigenvalues given in Eq. (12) are used to construct the generalized zeta function (9), which is written as,

$$\zeta(s) = \frac{\Omega_3}{(2\pi)^3} \sum_{n=1}^{\infty} \int dk_\tau dk_x dk_y \left\{ k_\tau^2 + (-1)^{2\xi} l^{2(\xi-1)} \left[ k_x^2 + k_y^2 + \left( \frac{\pi n}{L} \right)^2 \right]^\xi + V''(\Phi) \right\}^{-s}. \quad (13)$$

The quantity  $\Omega_3$  represents the 3-dimensional volume associated with the Euclidean time coordinate  $\tau$  and the spatial coordinates  $x$  and  $y$ . In order to obtain the generalized zeta function in a more convenient form, we start by using the following identity:

$$w^{-s} = \frac{2}{\Gamma(s)} \int_0^\infty dt t^{2s-1} e^{-wt^2}, \quad (14)$$

where  $\Gamma(s)$  is the gamma function. This allows us to perform the Gaussian-like integral in the  $k_\tau$  variable present in Eq. (13), providing that,

$$\zeta(s) = \frac{2\Omega_3\pi^{\frac{1}{2}}}{(2\pi)^3\Gamma(s)} \sum_{n=1}^{\infty} \int dk_x dk_y \int_0^{\infty} dt t^{2s-2} \exp \left\{ -bt^2 \left[ \left( k_x^2 + k_y^2 + \left( \frac{\pi n}{L} \right)^2 \right)^\xi + \frac{V''(\Phi)}{b} \right] \right\}, \quad (15)$$

where we have defined the quantity  $b$  as,

$$b = l^{2(\xi-1)}. \quad (16)$$

At this stage, it is more appropriate to write the  $k_x$  and  $k_y$  integrals in polar coordinates and perform the integral in the polar angle. After we perform two changes of integration variables, namely,  $\chi = \frac{b\pi^{2\xi}}{L^{2\xi}} t^2$  and  $\omega = \chi \left[ \left( \frac{kL}{\pi} \right)^2 + n^2 \right]^\xi$ , we end up with the following expression for the generalized zeta function:

$$\zeta(s) = \frac{\Omega_3 b^{\frac{1}{2}-s} \pi^{\frac{1}{2}-2\xi s+\xi}}{8\xi L^{2-2\xi s+\xi} \Gamma(s)} \sum_{n=1}^{\infty} \int_0^{\infty} d\chi \chi^{s-\frac{3}{2}-\frac{1}{\xi}} e^{-\chi U} \int_{\chi n^{2\xi}}^{\infty} d\omega \omega^{\frac{1}{\xi}-1} e^{-\omega}, \quad (17)$$

where we set  $U$  in the form,

$$U = \frac{L^{2\xi}}{b\pi^{2\xi}} V''(\Phi). \quad (18)$$

In the generalized zeta function given in Eq. (17), we identify the incomplete gamma function  $\Gamma(\alpha, x)$  defined as [43],

$$\Gamma(\alpha, x) = \int_x^{\infty} dt t^{\alpha-1} e^{-t} = e^{-x} \Psi(1-\alpha, 1-\alpha, x), \quad \text{Re } \alpha > 0, \quad (19)$$

where the function  $\Psi(\alpha, \beta, z)$  is a combination of confluent hypergeometric functions  ${}_1F_1(\alpha, \gamma, z)$  [43], that is,

$$\Psi(\alpha, \beta, z) = \frac{\Gamma(1-\gamma)}{\Gamma(\alpha-\gamma+1)} {}_1F_1(\alpha, \gamma, z) + \frac{\Gamma(1-\gamma)}{\Gamma(\alpha)} z^{1-\gamma} {}_1F_1(\alpha-\gamma+1, 2-\gamma, z). \quad (20)$$

Hence, we obtain the following expression for the generalized zeta function:

$$\zeta(s) = \frac{\Omega_3 b^{\frac{1}{2}-s} \pi^{\frac{1}{2}-2\xi s+\xi}}{8\xi \Gamma(s) L^{2-2\xi s+\xi}} \sum_{n=1}^{\infty} \int_0^{\infty} d\tau \frac{\tau^{s-\frac{3}{2}-\frac{1}{\xi}}}{n^{2\xi s-\xi-2}} e^{-\tau(1+\frac{U}{n^{2\xi}})} \Psi\left(1-\frac{1}{\xi}, 1-\frac{1}{\xi}, \tau\right), \quad (21)$$

where we have made another change of variable, namely,  $\tau = tn^{2\xi}$ . The form of the generalized zeta function above suggests the use of the integral below [43], i.e.,

$$\int_0^{\infty} t^{b-1} e^{-zt} \Psi(a, c, t) dt = \frac{\Gamma(b)\Gamma(b-c+1)z^{-b}}{\Gamma(a+b-c+1)} {}_2F_1(a, b, a+b-c+1, 1-z^{-1}). \quad (22)$$

Therefore, with the help of Eq. (22), we can rewrite the generalized zeta function, Eq. (21), as

$$\begin{aligned} \zeta(s) &= \frac{\Omega_3 \pi^{\frac{1}{2}-2\xi s+\xi} b^{\frac{1}{2}-s} \Gamma\left(s-\frac{1}{2}-\frac{1}{\xi}\right) \Gamma\left(s-\frac{1}{2}\right)}{8\xi L^{2-2\xi s+\xi} \Gamma(s) \Gamma\left(s+\frac{1}{2}-\frac{1}{\xi}\right)} \\ &\times \sum_{n=1}^{\infty} (n^{2\xi} + U)^{\frac{1}{2}+\frac{1}{\xi}-s} {}_2F_1\left(1-\frac{1}{\xi}, s-\frac{1}{2}-\frac{1}{\xi}, s+\frac{1}{2}-\frac{1}{\xi}, \frac{U}{n^{2\xi}+U}\right), \end{aligned} \quad (23)$$

where the function  ${}_2F_1(\alpha, \beta, \gamma, z)$  is the hypergeometric function [43]. The sum above is clearly divergent so that we need a renormalization method to subtract the infinite contribution and only work with the finite part of the generalized zeta function.

In order to perform the sum over the quantum number  $n$  in Eq. (23) and obtain a finite contribution, we use the Abel-Plana summation formula [13, 33, 44, 45]. The calculations using this formula are described in Appendix A

where it is shown that there are three resulting terms, but only one provides a finite vacuum energy density, which is given by

$$\zeta_0(s) = - \frac{\Omega_3 \pi^{\frac{1}{2} + \xi - 2\xi s} b^{\frac{1}{2} - s} \Gamma\left(s - \frac{1}{2} - \frac{1}{\xi}\right) \Gamma\left(s - \frac{1}{2}\right) \sin\left[\pi\left(\frac{\xi}{2} + 1 - \xi s\right)\right]}{4\xi L^{2+\xi-2\xi s} \Gamma(s) \Gamma\left(s + \frac{1}{2} - \frac{1}{\xi}\right)} \times \int_{U^{\frac{1}{2\xi}}}^{\infty} dx \mathcal{F}_s(\xi, U, x), \quad (24)$$

where we have defined the function  $\mathcal{F}_s(\xi, U, x)$  as

$$\mathcal{F}_s(\xi, U, x) = \frac{(x^{2\xi} - U)^{\frac{1}{2} + \frac{1}{\xi} - s}}{e^{2\pi x} - 1} {}_2F_1\left(1 - \frac{1}{\xi}, s - \frac{1}{2} - \frac{1}{\xi}, s + \frac{1}{2} - \frac{1}{\xi}, \frac{U}{U - x^{2\xi}}\right). \quad (25)$$

With the finite generalized zeta function obtained above, we proceed to calculate the one-loop correction to the effective potential from Eq. (10). In order to do so, we have to evaluate the generalized zeta function above and its derivative at  $s = 0$ , that is,  $\zeta(0)$  and  $\zeta'(0)$ . From the calculations presented in Appendix A, we find that,

$$\zeta_0(0) = 0, \quad \zeta'_0(0) = \frac{\Omega_3 \pi^{1+\xi} b^{\frac{1}{2}} \sin(\pi\xi/2)}{(\xi + 2) L^{2+\xi}} \int_{U^{\frac{1}{2\xi}}}^{\infty} dx \mathcal{F}_0(\xi, U, x), \quad (26)$$

where we should remember that the quantity  $U$  is given in Eq. (18) together with (8). We should also emphasize that the contribution presented in Eq. (26) is the one that gives rise to the vacuum energy density, as we shall see.

Due to the renormalization procedure performed using Abel-Plana summation formula [33], the one-loop correction to the effective potential takes into consideration only the contribution given in Eq. (26), therefore the one-loop correction, Eq. (10), is written in the following manner:

$$V^{(1)}(\Phi) = - \frac{\pi^{1+\xi} l^{\xi-1} \sin(\pi\xi/2)}{2(\xi + 2) L^{3+\xi}} \int_{U^{\frac{1}{2\xi}}}^{\infty} dx \mathcal{F}_0(\xi, U, x). \quad (27)$$

Hence, the renormalized effective potential for a massive self-interacting scalar field within the Hořava-Lifshitz formalism takes the form

$$V_{\text{eff}}^R(\Phi) = \frac{1}{2} m \Phi^2 + \frac{\lambda}{4!} \Phi^4 - \frac{\pi^{1+\xi} l^{\xi-1} \sin(\pi\xi/2)}{2(\xi + 2) L^{3+\xi}} \int_{U^{\frac{1}{2\xi}}}^{\infty} dx \mathcal{F}_0(\xi, U, x). \quad (28)$$

Once we obtain the explicit form of the renormalized effective potential, up to one-loop correction, we can calculate the vacuum energy density and also analyze a possible generation of topological mass. Let us do this in the proceeding sections.

#### IV. VACUUM ENERGY DENSITY AND TOPOLOGICAL MASS

In this section we investigate the vacuum energy density for a real scalar field, its corresponding order  $\lambda$  correction, which is in fact the contribution from the two-loop correction to the effective potential calculated at the vacuum state, and also the topological mass. Next, we consider first the vacuum energy density.

##### A. Vacuum energy density for the massive field

Upon using the renormalized effective potential (28) obtained in the previous section, we can calculate the vacuum energy density directly by taking the vacuum state, i.e.,  $\Phi = 0$ . Hence, we obtain the vacuum energy density in the following form:

$$\begin{aligned} \mathcal{E}_0 &= V_{\text{eff}}^R(0) \\ &= - \frac{\pi \sin(\pi\xi/2)}{2L^4 (\xi + 2) R_\xi} \int_{U_0^{\frac{1}{2\xi}}}^{\infty} dx \mathcal{F}_0(\xi, U_0, x), \end{aligned} \quad (29)$$

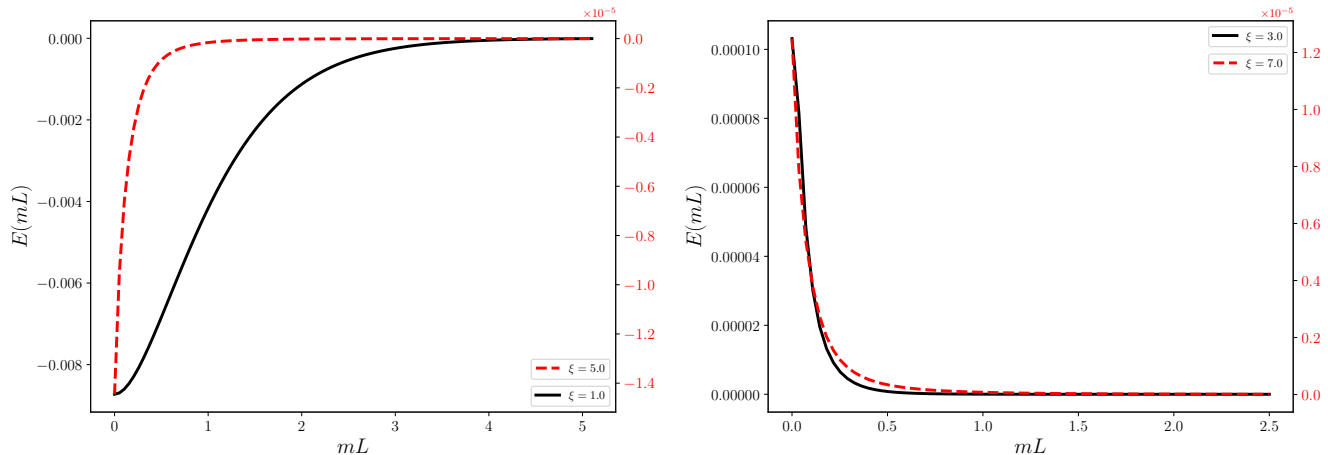


FIG. 1: Graphs of the dimensionless vacuum energy density  $E(mL) = \frac{4}{\pi}L^4\mathcal{E}_0$ , as a function of  $mL$ . The graph on the left considers the values  $\xi = 1.0$  (solid black curve) and  $\xi = 5.0$  (dashed red curve), while the plot on the right considers the values  $\xi = 3.0$  (solid black curve) and  $\xi = 7.0$  (dashed red curve). The scale of each curve is shown in the vertical axes with the correspondent color.

where the function  $\mathcal{F}_0(\xi, U_0, x)$  is presented in Eq. (25), with  $U_0$  given by,

$$\begin{aligned} U_0 = U|_{\Phi=0} &= (mL)^2 \left[ \frac{1}{\pi^\xi} \left( \frac{L}{l} \right)^{\xi-1} \right]^2 \\ &= (mL)^2 R_\xi^2. \end{aligned} \quad (30)$$

As we can see, the vacuum energy density given in Eq. (29) can be positive or negative depending on the value of the parameter  $\xi$  which, as seen in Appendix A, assumes only odd values. The expression (29) is the general result for the vacuum energy density, for a massive scalar field within the Hořava-Lifshitz formalism, satisfying Dirichlet boundary conditions on the parallel plates. Unfortunately, it is not possible to solve the integral in Eq. (29) for all odd values of  $\xi$ , except the standard case  $\xi = 1$  that preserves the Lorentz symmetry.

Let us now closely consider the standard case in which the critical exponent is set equal to the unity, i.e.,  $\xi = 1$ . Since  $F(0, \beta, \gamma, x) = 1$ , the vacuum energy density in Eq. (29) becomes

$$\mathcal{E}_0(\xi = 1) = -\frac{m^4}{6\pi^2} \sum_{n=1}^{\infty} \int_1^{\infty} dy (y^2 - 1)^{\frac{3}{2}} e^{-2nmLy}, \quad (31)$$

where we have performed the change of integration variable,  $y = xU_0^{-\frac{1}{2}}$ . Note also that the sum in  $n$  of the exponential above provides the expression  $(e^{2mLy} - 1)^{-1}$ .

The integral in Eq. (31) can be performed with the help of the following identity [43]:

$$\int_1^{\infty} dx (x^2 - 1)^{\nu-1} e^{-\mu x} = \pi^{-\frac{1}{2}} \left( \frac{2}{\mu} \right)^{\nu-\frac{1}{2}} \Gamma(\nu) K_{\nu-\frac{1}{2}}(\mu), \quad (32)$$

where  $K_2(\mu)$  is the Macdonald function or the modified Bessel function of the second kind [46]. Hence, the vacuum energy density for the case  $\xi = 1$  takes the form,

$$\mathcal{E}_0(\xi = 1) = -\frac{m^2}{8\pi^2 L^2} \sum_{n=1}^{\infty} n^{-2} K_2(2nmL). \quad (33)$$

The above result is in agreement with the standard result where the Lorentz symmetry is preserved which we can check, for instance, in Refs. [14, 47, 48].

In order to construct a graph for the vacuum energy density given in Eq. (29) as a function of  $mL$ , it is more convenient to express it in terms of the variable,  $z = x^{2\xi} - U$ . Hence, Eq. (29) can be written as

$$\mathcal{E}_0 = -\frac{\pi \sin(\pi\xi/2)}{4L^4\xi(\xi+2)R_\xi} \int_0^\infty dz \frac{z^{\frac{1}{2}+\frac{1}{\xi}}(z+U_0)^{\frac{1}{2\xi}-1}}{\left[e^{2\pi(z+U_0)^{\frac{1}{2\xi}}} - 1\right]} {}_2F_1\left(1 - \frac{1}{\xi}, -\frac{1}{2} - \frac{1}{\xi}, \frac{1}{2} - \frac{1}{\xi}, -\frac{U_0}{z}\right), \quad (34)$$

where  $U_0$  has been defined in terms of  $R_\xi$  in Eq. (30). Thus, we shall now consider graphs of the dimensionless vacuum energy density,  $E(mL) = \frac{4L^4}{\pi}\mathcal{E}_0$ , as a function of  $mL$ .

In Fig.1 we exhibit graphs of the dimensionless vacuum energy density  $E(mL)$ , as a function of  $mL$ , considering the values  $\xi = 1, 3, 5, 7$ . The graph on the left shows the curves for  $\xi = 1$  and  $\xi = 5$ . The solid black curve stands for the case  $\xi = 1$  while the dashed red curve for the case  $\xi = 5$ . Similarly, the graph on the right considers the cases where  $\xi = 3$  (solid black line) and  $\xi = 7$  (dashed red line). Note that the scale of each curve is correspondently shown on the left and on the right of the vertical axes. Although in section IV D we make an estimation on the ratio  $\frac{1}{L}$  by using experimental data, for simplicity, we have taken values of  $R_\xi$  such that

$$R_1 = 1/\pi, \quad R_3 = 24, \quad R_5 = 32, \quad R_7 = 80, \quad R_9 = 260. \quad (35)$$

Therefore, the plot on the left of Fig.1 shows that the order of the vacuum energy density, in absolute values, greatly decreases compared with the standard case  $\xi = 1$ . This aspect is also shown in the plot on the right, which also reveals that for values  $\xi = 3, 7$  the vacuum energy density gives rise to a repulsive force, in contrast with the cases  $\xi = 1, 5$ .

Let us now consider the massless scalar field case. For this, we should take the limit  $m \rightarrow 0$  ( $U_0 \rightarrow 0$ ) in Eq. (29). This provides

$$\mathcal{E}_0 = -\frac{\pi^{1+\xi}l^{(\xi-1)}\sin(\pi\xi/2)}{2(\xi+2)L^{3+\xi}} \int_0^\infty \frac{x^{\xi+2}}{e^{2\pi x} - 1} dx. \quad (36)$$

The integral above can be performed by using the following relation [43]:

$$\int_0^\infty dx \frac{x^{\nu-1}}{e^{\mu x} - 1} = \mu^{-\nu}\Gamma(\nu)\zeta_R(\nu), \quad \mu > 0, \quad \nu > 1, \quad (37)$$

where  $\zeta_R(s)$  is the Riemann zeta function. Therefore, we obtain the vacuum energy density for the massless field as

$$\mathcal{E}_0 = -\frac{l^{(\xi-1)}\sin(\pi\xi/2)}{2^{\xi+4}\pi^2L^{3+\xi}}\Gamma(\xi+2)\zeta_R(\xi+3), \quad (38)$$

which is in agreement with the result found in Ref. [33].

We want now go further to consider the correction to the vacuum energy density, which is proportional to the self-interaction coupling constant  $\lambda$ , in linear order. This contribution comes from the two-loop correction to the effective potential, as we shall see below.

## B. Order- $\lambda$ correction to the vacuum energy density

The two-loop correction to the effective potential at the vacuum state  $\Phi = 0$ , provides a order- $\lambda$  loop correction to the vacuum energy density, Eq. (29). This contribution can be written in terms of the finite generalized zeta function (24) as [18, 40, 41],

$$\mathcal{E}_0^\lambda = V^{(2)}(0) = \frac{\lambda}{8} \left[ \frac{\zeta_0(1)}{\Omega_4} \right]_{\Phi=0}^2, \quad (39)$$

where

$$\frac{\zeta_0(1)}{\Omega_4} \Big|_{\Phi=0} = -\frac{\pi^{1-\xi}\sin(\pi\xi/2)}{2(\xi-2)l^{(\xi-1)}L^{3-\xi}} \int_{U_0^{\frac{1}{2\xi}}}^\infty dx \mathcal{F}_1(\xi, U_0, x), \quad (40)$$

with  $\Omega_4 = \Omega_3 L$ . This leads to the following order- $\lambda$  correction to the vacuum energy density:

$$\mathcal{E}_0^\lambda = \frac{\lambda\pi^2 R_\xi^2}{32L^4(\xi-2)^2} \left[ \int_{U_0^{\frac{1}{2\xi}}}^\infty dx \mathcal{F}_1(\xi, U_0, x) \right]^2, \quad (41)$$

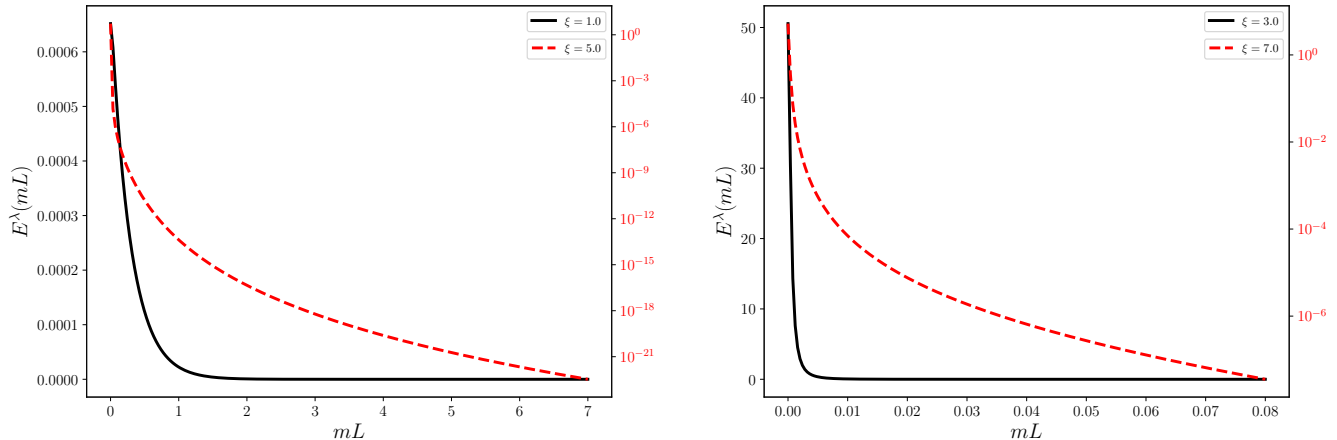


FIG. 2: Graphs of the dimensionless order- $\lambda$  contribution to the vacuum energy density  $E^\lambda(mL) = \frac{128}{\lambda\pi^2} L^4 \mathcal{E}_0^\lambda$ , as a function of  $mL$ . The graph on the left considers the values  $\xi = 1.0$  (solid black curve) and  $\xi = 5.0$  (dashed red curve), while the plot on the right considers the values  $\xi = 3.0$  (solid black curve) and  $\xi = 7.0$  (dashed red curve). The scale of each curve is shown in the vertical axes with the correspondent color.

where  $R_\xi$  has been defined in Eq. (30) and the function  $\mathcal{F}_s(\xi, U_0, x)$  in Eq. (25). In order to construct a graph for the above correction it is useful to use the same change of variable as in Eq. (34).

In Fig.2 we have plotted the dimensionless order- $\lambda$  correction to the vacuum energy density  $E^\lambda(mL) = \frac{128}{\lambda\pi^2} L^4 \mathcal{E}_0^\lambda$  as a function of  $mL$ . The graph on the left considers the case  $\xi = 1$  represented by the solid black curve, while the case  $\xi = 5$  is represented by the dashed red curve. Similarly, the graph on the right shows the cases  $\xi = 3$  (solid black curve) and  $\xi = 7$  (dashed red curve). For both plots, the scale of the vacuum energy density is shown in the vertical axes with the correspondent color. Note that in both plots the red vertical axis is in logarithmic scale. Note also that the values given in Eq. (35) are also considered here. We can again see that the scale of the vacuum energy density greatly decreases in each case, as compared with the standard case  $\xi = 1$ . The graphs above also show that the correction to the vacuum energy density goes to zero as  $mL \rightarrow \infty$ . However, exactly at  $mL = 0$  (massless case), the correction diverges for  $\xi > 1$ , as we shall see more clearly below.

We turn now to the massless scalar field case, which can be obtained by taking the limit  $m \rightarrow 0$  ( $U_0 \rightarrow 0$ ) of Eq. (41). This gives

$$\mathcal{E}_0^\lambda = \frac{\lambda\pi^{2-2\xi}}{32(\xi-2)^2 l^{2(\xi-1)} L^{6-2\xi}} \left[ \int_0^\infty dx \frac{x^{2-\xi}}{e^{2\pi x} - 1} \right]^2. \quad (42)$$

Note that the integral above does not converge for  $\xi > 1$ . This is a consequence of the Hořava-Lifshitz model adopted here, which helps to eliminate ultraviolet divergences but as a consequence brings infrared ones in the massless limit of Eq. (41). The question whether this infrared divergence can be treated will be considered elsewhere.

Fortunately, the integral in Eq. (42) converges for  $\xi = 1$  and provides the standard result where the Lorentz symmetry is preserved [39]. So, let us first consider  $\xi = 1$  in Eq. (41). In this case, we obtain the following result:

$$\begin{aligned} \mathcal{E}_0^\lambda(\xi = 1) &= \frac{\lambda m^4}{32\pi^4} \left[ \sum_{n=1}^{\infty} \int_1^{\infty} dy (y^2 - 1)^{\frac{1}{2}} e^{-2nmLy} \right]^2 \\ &= \frac{\lambda m^2}{128\pi^4 L^2} \left[ \sum_{n=1}^{\infty} n^{-1} K_1(2nmL) \right]^2, \end{aligned} \quad (43)$$

which is in agreement with the results found in Ref. [39] in the case with no Lorentz violation. Note that we have used again the change of variable  $y = xU_0^{-\frac{1}{2}}$ , and also Eq. (32). This is similar to what we have done in Eq. (31).

In addition, from Eq. (42), for a massless scalar field, we have

$$\mathcal{E}_0^\lambda(\xi = 1) = \frac{\lambda}{18432L^4}, \quad (44)$$



which is also in agreement with Ref. [39].

In the next section we consider an analysis for the topological mass generated by the boundary condition. We, thus, expect the result will depend on the self-interaction coupling  $\lambda$  and the Lorentz violation parameter  $l$ .

### C. Topological mass for the massive field

In this section we investigate the topological mass which arises due to the boundary condition, self-interaction potential and the Lorentz violation within the Hořava-Lifshitz formalism used here.

The topological mass squared of the field can be written as the second derivative of the effective potential, evaluate at the vacuum state, that is,  $\Phi = 0$  [38]. Hence, using the effective potential given in Eq. (28) we write the topological mass as,

$$m_{\text{T}}^2 = \left. \frac{d^2 V_{\text{eff}}^{\text{R}}(\Phi)}{d\Phi^2} \right|_{\Phi=0}. \quad (45)$$

In order to perform the derivative of the effective potential, we have to apply the Leibniz rule [49]. The final result reads,

$$m_{\text{T}}^2 = m^2 - \frac{\lambda\pi \sin(\pi\xi/2)}{4\xi L^4 m^2 R_\xi} \int_{U_0^{-\frac{1}{2\xi}}}^{\infty} dx \left[ \mathcal{F}_0(\xi, U_0, x) - \frac{x^2 (x^{2\xi} - U_0)^{\frac{1}{2}}}{e^{2\pi x} - 1} \right]. \quad (46)$$

The expression above, as expected, goes to zero as  $mL \rightarrow \infty$  for any odd value of  $\xi$ . However, at  $mL = 0$ , that is, in the massless case, it diverges for  $\xi > 1$  as a consequence of infrared divergences that appear due to the Hořava-Lifshitz model adopted here. This problem, on the other hand, does not exist if we take  $\xi = 1$ , which is the standard case where the Lorentz symmetry is preserved. Hence, for  $\xi = 1$ , Eq. (46) can be written as

$$m_{\text{T}}^2 = m^2 + \frac{\lambda m^2}{4\pi^2} \sum_{n=1}^{\infty} \int_1^{\infty} dy (y^2 - 1)^{\frac{1}{2}} e^{-2nmLy}, \quad (47)$$

where we have expressed  $(e^{2\pi x} - 1)^{-1}$  as a sum in  $n$  of the exponential above. We have also performed the change of variable  $y = xU_0^{-\frac{1}{2}}$ , similar to Eq. (31). Now, by using Eq. (32) we find

$$m_{\text{T}}^2(\xi = 1) = m^2 \left[ 1 + \frac{\lambda}{8\pi^2 mL} \sum_{n=1}^{\infty} n^{-1} K_1(2nmL) \right], \quad (48)$$

which is in agreement with known results found in the literature [39]. Note that the massless scalar field case for the topological mass follows directly from Eq. (48).

Nevertheless, in order to better notice the infrared divergences that appear in the massless limit of Eq. (46), let us take the limit  $mL \rightarrow 0$  ( $U_0 \rightarrow 0$ ) of Eq. (46). For this, we should consider the following expansion for small  $mL$ :

$$\left[ (e^{2\pi x} - 1) \mathcal{F}_0(\xi, U_0, x) - x^2 (x^{2\xi} - U_0)^{\frac{1}{2}} \right] \simeq \frac{\xi x^{2-\xi}}{(\xi - 2)} U_0 + O(U_0^2). \quad (49)$$

Consequently, Eq. (46) becomes

$$m_{\text{T}}^2 = -\frac{\lambda\pi \sin(\pi\xi/2) R_\xi}{4(\xi - 2) L^2} \int_0^{\infty} \frac{dx x^{2-\xi}}{(e^{2\pi x} - 1)}. \quad (50)$$

As we can see, the integral above does not converge for  $\xi > 1$ . However, for  $\xi = 1$ , we have

$$m_{\text{T}}^2(\xi = 1) = \frac{\lambda}{96L^2}, \quad (51)$$

which is a known result [39]. It is clear now that, for any odd values of  $\xi$ , the expression in Eq. (46) is only valid for  $m > 0$ . On the other hand, for  $\xi = 1$ , it provides known results for both the massive and massless scalar field cases.

In order to plot the expression in Eq. (46) with respect to  $mL$  it is again useful to use the same change of variable as in Eq. (34). The correspondent plots are exhibited in Fig.3. Note that we have plotted only the second term on the r.h.s. of Eq. (46). The graphs clearly show that the topological mass goes to zero as  $mL \rightarrow \infty$ , as it should be. However, for  $mL \rightarrow 0$ , the topological mass goes to infinity indicating the presence of infrared divergences in the massless limit. Moreover, as we can see, for some values of  $\xi$  like  $\xi = 5, 9$ , the values of the topological mass become negative which may indicate that an analysis of vacuum stability is necessary within a model where the scalar field considered here interacts with a second field, similar what has been done in Refs. [41, 50].

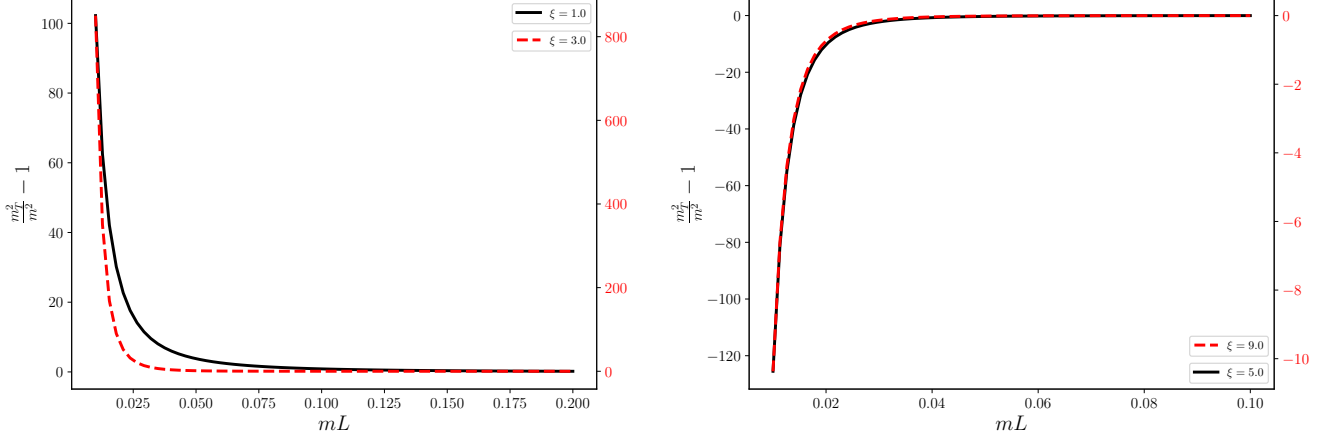


FIG. 3: Graphs of the dimensionless topological mass  $\frac{m_l^2}{m^2} - 1$ , as a function of  $mL$ . The graph on the left considers the values  $\xi = 1.0$  (solid black curve) and  $\xi = 3.0$  (dashed red curve), while the plot on the right considers the values  $\xi = 5.0$  (solid black curve) and  $\xi = 9.0$  (dashed red curve). The scale of each curve is shown in the vertical axes with the correspondent color.

#### D. Estimative for the ratio $(l/L)^{\xi-1}$

In this section we consider the experimental results presented in [3] in order to estimate the ratio  $(l/L)^{\xi-1}$ . Hence, from Ref. [3], we consider

$$\Delta\nu^2 = -\frac{C_{\text{Cas}}}{L^5}, \quad (52)$$

where  $C_{\text{Cas}} = (2.34 \pm 0.34) \times 10^{-28} \text{ Hz}^2\text{m}^5$ . The connection between the vacuum energy density given in Eq. (38), with the Casimir energy  $E_0$  is given by [39],

$$E_0 = AL\mathcal{E}_0, \quad (53)$$

where  $A$  is the area of the plates. The Casimir force,  $F_0$ , is obtained via derivative of the Casimir energy with respect to the distance  $L$ , and the Casimir pressure,  $P_0$ , is the Casimir force divided by the area  $A$ , i.e.,

$$P_0 = \frac{F_0}{A} = -\frac{1}{A} \frac{\partial E_0}{\partial L}. \quad (54)$$

According to the method proposed in Ref. [51], we can write the relation between  $\Delta\nu^2$  and  $E_0$  as,

$$\Delta\nu^2 = -\frac{A}{4\pi^2 m_{\text{eff}}} \frac{\partial P_0}{\partial L} = \frac{A}{4\pi^2 m_{\text{eff}}} \frac{\partial}{\partial L} \left( \frac{1}{A} \frac{\partial E_0}{\partial L} \right), \quad (55)$$

where  $m_{\text{eff}}$  is an effective mass and the ratio  $A/m_{\text{eff}}$  is experimentally estimated in [3], that is,

$$\frac{A}{m_{\text{eff}}} \approx 1.746 \text{ Hz}^2\text{m}^3\text{N}^{-1}. \quad (56)$$

Using the result obtained in Eq. (38) for the vacuum energy density in the case of massless scalar field, together with the relation expressed by Eq. (53), we find the Casimir pressure for a massless field in the Hořava-Lifshitz model considered here as

$$P_0 = -\sin\left(\frac{\pi\xi}{2}\right) \frac{(2+\xi)l^{(\xi-1)}}{2^{\xi+4}\pi^2} \Gamma(\xi+2) \zeta_R(\xi+3) \frac{1}{L^{3+\xi}}. \quad (57)$$

Therefore the quantity  $\Delta\nu^2$  given in Eq. (55) can be written in the form,

$$\Delta\nu^2 = -\frac{A}{m_{\text{eff}}} \sin\left(\frac{\pi\xi}{2}\right) \frac{(3+\xi)(2+\xi)}{2^{\xi+6}\pi^4} \Gamma(\xi+2) \zeta_R(\xi+3) \left(\frac{l}{L}\right)^{\xi-1} \frac{1}{L^5}. \quad (58)$$

$\xi$	$\xi = 3$	$\xi = 5$	$\xi = 7$	$\xi = 9$
$(\frac{l}{L})^{\xi-1}$	$(\frac{l}{L})^2 = 1.32588 \times 10^{-27}$	$(\frac{l}{L})^4 = 9.59569 \times 10^{-29}$	$(\frac{l}{L})^6 = 4.27789 \times 10^{-30}$	$(\frac{l}{L})^8 = 1.2973 \times 10^{-31}$

TABLE I:  $(l/L)^{\xi-1}$  as a function of  $\xi$ .

Considering the estimated result written in Eq. (56), together with the Eq. (52), we write the ratio  $(l/L)^{\xi-1}$  in the following way

$$\left(\frac{l}{L}\right)^{\xi-1} = 0.34 \times 10^{-28} \frac{m_{\text{eff}}}{A} \frac{2^{\xi+6} \pi^4}{(3+\xi)(2+\xi) \sin\left(\frac{\pi\xi}{2}\right) \Gamma(\xi+2) \zeta_R(\xi+3)}, \quad (59)$$

where we have considered the error bar of  $C_{\text{Cas}}$ . Hence, from the experimental value of  $A/m_{\text{eff}}$  written in Eq. (56), the expression in Eq. (59) allows us to construct Table I. Note that we are taking the absolute value of the ratio  $l/L$ , since it is a positive quantity. As we can see from Table I, the bigger the value of  $\xi$  the smaller the ratio  $l/L$ . The biggest value is for  $\xi = 3$ , which is about  $l/L \simeq 3.6 \times 10^{-14}$ .

## V. CONCLUDING REMARKS

Loop correction to the vacuum energy density and generation of topological mass have been considered for a system of a massive self-interacting scalar field in the context of a Hořava-Lifshitz model. The vacuum energy density and topological mass arise not only from the Dirichlet boundary condition adopted, but also from the Lorentz violation associated with the Hořava-Lifshitz model. The formalism used in our investigation is the effective potential one, which is written as a loop expansion.

The vacuum energy density,  $\mathcal{E}_0$ , for a massive scalar field in the Hořava-Lifshitz model considered and under Dirichlet boundary condition has been obtained in Eq. (29), which depends on the distance between the plates  $L$  and also on the critical exponent  $\xi$ , associated with the Hořava-Lifshitz model. It has been shown that the vacuum energy density vanishes in the cases where  $\xi$  is an even number. Unfortunately, an analytical expression is not possible for general values of  $\xi$ , that is,  $\xi \neq 1$ . However, in Fig.1 we have exhibited the graphs of the dimensionless vacuum energy density  $E(mL) = 4\pi^2 L^4 \mathcal{E}_0$ , as a function of  $mL$ , considering the values  $\xi = 1, 3, 5, 7$ . Additionally, the vacuum energy density for the case of a massless field is presented in Eq. (38), which shows the dependency on  $L$  and  $\xi$ , and reproduces the obtained results in Ref. [33]. A two-loop correction to the effective potential in the vacuum state  $\Phi = 0$  has been obtained, which provides a order- $\lambda$  correction to the vacuum energy density and is given by Eq. (41) for the massive field. Its massless limit, on the other hand, has been obtained in Eq. (42) and only gives a finite result for  $\xi = 1$ , the standard case where the Lorentz symmetry is preserved. For vales such that  $\xi > 1$  the integral does not converge as a consequence of infrared divergences introduced by the model. In Fig.2 we have exhibited graphs for the dimensionless two-loop contribution to the vacuum energy density  $\Delta E(mL) = \frac{128}{\lambda\pi^2} L^4 \mathcal{E}_0^\lambda$  as a function of  $mL$ , considering the values  $\xi = 1, 3, 5, 7$ . The graphs show that the correction goes to zero as  $mL \rightarrow \infty$  (as it should be) and diverges as  $mL \rightarrow 0$  (for  $\xi > 1$ ), indicating the infrared divergences.

In the case of a massive field, its mass acquires a correction which depends on the critical exponent,  $\xi$ , on the parameter  $L$  and also on the self-interaction coupling constant  $\lambda$ . This correction is presented in Eq. (46). However, for  $\xi > 1$ , this expression for the topological mass diverges as  $mL \rightarrow 0$ , also indicating the presence of infrared divergences. This can be better seen in Eq. (50), which clearly converges only for  $\xi = 1$ . In contrast, for  $mL \rightarrow \infty$  the topological mass goes to zero, as expected. This is shown in the graphs of Fig.3. The graph on the right shows that for  $\xi = 5, 9$  the topological mass is negative and a vacuum stability analysis must take place in a model with interacting fields.

We have also provided an estimative for the ratio  $l/L$  by comparison with experimental results presented in Ref. [3]. The values of the ratio  $l/L$  are presented in Table I. It shows that the ratio  $l/L$  decreases as  $\xi$  increases, with the biggest value being about  $l/L \simeq 3.6 \times 10^{-14}$ . As a future work, we plan to look further into the issue of infrared divergences that appear in the massless scalar field case, and also analyze a system where two scalar fields interact.

## Acknowledgments

The author H.M. is partially supported by the Brazilian agency National Council for Scientific and Technological Development (CNPq) under Grant No. 308049/2023-3.

### Appendix A: Abel-Plana formula

In this appendix we use the Abel-Plana formula [13, 33, 44, 45],

$$\sum_{n=1}^{\infty} f(n) = \int_0^{\infty} dx f(x) - \frac{1}{2}f(0) + i \int_0^{\infty} dx \frac{f(ix) - f(-ix)}{e^{2\pi x} - 1}, \quad (\text{A.1})$$

to perform the sum in  $n$  present in Eq. (23). Hence, the generalized zeta function in Eq. (23) can be written as a sum of three contributions, namely,

$$\zeta(s) = \zeta_{\text{M}}(s) + \zeta_{\text{IP}}(s) + \zeta_0(s). \quad (\text{A.2})$$

The first contribution,  $\zeta_{\text{M}}(s)$ , reads,

$$\begin{aligned} \zeta_{\text{M}}(s) &= \frac{\Omega_3 \pi^{\frac{1}{2} + \xi - 2\xi s}}{8\xi b^{s - \frac{1}{2}} L^{2 + \xi - 2\xi s}} \frac{\Gamma\left(s - \frac{1}{2} - \frac{1}{\xi}\right) \Gamma\left(s - \frac{1}{2}\right)}{\Gamma(s) \Gamma\left(s + \frac{1}{2} - \frac{1}{\xi}\right)} \\ &\times \int_0^{\infty} dx (x^{2\xi} + U)^{\frac{1}{2} + \frac{1}{\xi} - s} {}_2F_1\left(1 - \frac{1}{\xi}, s - \frac{1}{2} - \frac{1}{\xi}, s + \frac{1}{2} - \frac{1}{\xi}, \frac{U}{x^{2\xi} + U}\right), \end{aligned} \quad (\text{A.3})$$

which is in fact the Minkowski contribution that comes from the integral in the first term on r.h.s. of Eq. (A.1). The second contribution comes from the second term on r.h.s. of Eq. (A.1) and is associated with the one plate case. This contribution is given by

$$\begin{aligned} \zeta_{\text{IP}}(s) &= -\frac{\Omega_3 \pi^{\frac{1}{2} + \xi - 2\xi s} U^{\frac{1}{2} + \frac{1}{\xi} - s}}{16\xi b^{s - \frac{1}{2}} L^{2 + \xi - 2\xi s}} \frac{\Gamma\left(s - \frac{1}{2}\right)}{\Gamma(s)} \\ &\times \frac{\Gamma\left(s - \frac{1}{2} - \frac{1}{\xi}\right)}{\Gamma\left(s + \frac{1}{2} - \frac{1}{\xi}\right)} {}_2F_1\left(1 - \frac{1}{\xi}, s - \frac{1}{2} - \frac{1}{\xi}, s + \frac{1}{2} - \frac{1}{\xi}, 1\right). \end{aligned} \quad (\text{A.4})$$

For the third contribution we have to separate the integral in the variable  $x$  into two intervals: from  $[0, U^{\frac{1}{2\xi}}]$  and from  $[U^{\frac{1}{2\xi}}, \infty)$ . For the first interval and considering  $\xi$  an integer number, there is no contribution. In the second interval and considering  $\xi$  an integer number, the situation is more delicate. In this case we have  $U^{\frac{1}{2\xi}} < x$ , which yields,

$$\begin{aligned} f(ix) - f(-ix) &= 2i \sin\left(\frac{\pi\xi}{2} + \pi - \pi\xi s\right) \left[x^{2\xi} + (-1)^\xi U\right]^{\frac{1}{2} + \frac{1}{\xi} - s} \\ &\times {}_2F_1\left(1 - \frac{1}{\xi}, s - \frac{1}{2} - \frac{1}{\xi}, s + \frac{1}{2} - \frac{1}{\xi}, \frac{U}{U + (-1)^\xi (x)^{2\xi}}\right). \end{aligned} \quad (\text{A.5})$$

From the above expression we can infer that for  $\xi$  even, the difference above goes to zero, since we will eventually have to take  $s \rightarrow 0$ . Additionally, since the third term in the Abel-Plana formula is the one which originates the vacuum energy density, we see that for  $\xi$  even we have a vanishing vacuum energy density. Hence, we will investigate only the cases in which  $\xi$  is an odd number. Thus, for the third contribution in Eq. (A.2) that comes from the integral in the third term on the r.h.s. of Eq. (A.1), we have

$$\begin{aligned} \zeta_0(s) &= -\frac{\Omega_3 \sin\left[\pi\left(\frac{\xi}{2} + 1 - \xi s\right)\right]}{4\xi \pi^{2\xi s - \frac{1}{2} - \xi} b^{s - \frac{1}{2}} L^{2 + \xi - 2\xi s}} \frac{\Gamma\left(s - \frac{1}{2} - \frac{1}{\xi}\right) \Gamma\left(s - \frac{1}{2}\right)}{\Gamma(s) \Gamma\left(s + \frac{1}{2} - \frac{1}{\xi}\right)} \\ &\times \int_{U^{\frac{1}{2\xi}}}^{\infty} dx \frac{(x^{2\xi} - U)^{\frac{1}{2} + \frac{1}{\xi} - s}}{e^{2\pi x} - 1} {}_2F_1\left(1 - \frac{1}{\xi}, s - \frac{1}{2} - \frac{1}{\xi}, s + \frac{1}{2} - \frac{1}{\xi}, \frac{U}{U - x^{2\xi}}\right). \end{aligned} \quad (\text{A.6})$$

Thus, we have the generalized zeta function, Eq. (A.2), as a sum of three terms, namely, Eq. (A.3), (A.4) and (A.6).

The next step is to evaluate the generalized zeta function and its derivatives at  $s = 0$ , for each of the three terms separately. All the three terms are zero at  $s = 0$ , and by series expansion about  $s = 0$  we obtain the derivatives as

$$\begin{aligned}\zeta'_M(0) &= \frac{\Omega_3 \pi^{\xi+1} b^{\frac{1}{2}} U^{\frac{1}{2} + \frac{3}{2\xi}}}{4(\xi+2)L^{\xi+2}} \int_0^\infty dy (y^{2\xi} + 1)^{\frac{1}{2} + \frac{1}{\xi}} F\left(1 - \frac{1}{\xi}, -\frac{1}{2} - \frac{1}{\xi}, \frac{1}{2} - \frac{1}{\xi}, \frac{1}{1+y^{2\xi}}\right), \\ \zeta'_{1P}(0) &= -\frac{\Omega_3 \pi^{\xi + \frac{1}{2}} b^{\frac{1}{2}} U^{\frac{1}{2} + \frac{1}{\xi}}}{16\xi b^{\frac{1}{\xi}} L^{\xi+2}} \Gamma\left(-\frac{1}{2} - \frac{1}{\xi}\right) \Gamma\left(\frac{1}{\xi}\right), \\ \zeta'_0(0) &= \sin\left(\frac{\pi\xi}{2}\right) \frac{\Omega_3 \pi^{1+\xi} b^{\frac{1}{2}}}{(\xi+2)L^{2+\xi}} \sum_{n=1}^{\infty} \int_{U^{\frac{1}{2\xi}}}^{\infty} dx \mathcal{F}(n, \xi, U, x).\end{aligned}\tag{A.7}$$

Note that in the first line of the above equation, we change the integration variable as  $y^{2\xi} = x^{2\xi}/U$ . Besides, this term is divergent and represents the contribution with no boundaries (no parallel plates, that is, the Minkowski contribution) and it should be discarded [33]. The contribution from the second line of the above equation is the contribution coming from one plate, which grows with positive powers of the mass present in  $U$  (see Eq. (30)) and, thus should be discarded. Finally, the third line gives the contribution which truly generates the vacuum energy density.

- 
- [1] H. B. Casimir, *On the attraction of two perfectly conducting plates*, in *Proc. Kon. Ned. Akad. Wet.*, vol. 51, p. 793, 1948.
  - [2] M. J. Sparnaay, *Measurements of attractive forces between flat plates*, *Physica* **24** (1958) 751–764.
  - [3] G. Bressi, G. Carugno, R. Onofrio, and G. Ruoso, *Measurement of the casimir force between parallel metallic surfaces*, *Phys. Rev. Lett.* **88** (Jan, 2002) 041804.
  - [4] W. J. Kim, M. Brown-Hayes, D. A. R. Dalvit, J. H. Brownell, and R. Onofrio, *Anomalies in electrostatic calibrations for the measurement of the casimir force in a sphere-plane geometry*, *Phys. Rev. A* **78** (Aug, 2008) 020101.
  - [5] S. K. Lamoreaux, *Demonstration of the casimir force in the 0.6 to 6 $\mu$ m range*, *Phys. Rev. Lett.* **78** (Jan, 1997) 5–8.
  - [6] S. Lamoreaux, *Erratum: Demonstration of the casimir force in the 0.6 to 6  $\mu$  m range [phys. rev. lett. 78, 5 (1997)]*, *Physical Review Letters* **81** (1998), no. 24 5475.
  - [7] U. Mohideen and A. Roy, *Precision measurement of the Casimir force from 0.1 to 0.9 micrometers*, *Phys. Rev. Lett.* **81** (1998) 4549–4552, [[physics/9805038](#)].
  - [8] V. M. Mostepanenko, *New experimental results on the casimir effect*, *Brazilian Journal of Physics* **30** (2000), no. 2 309–315.
  - [9] Q. Wei, D. A. R. Dalvit, F. C. Lombardo, F. D. Mazzitelli, and R. Onofrio, *Results from electrostatic calibrations for measuring the casimir force in the cylinder-plane geometry*, *Phys. Rev. A* **81** (May, 2010) 052115.
  - [10] A. Romeo and A. A. Saharian, *Casimir effect for scalar fields under Robin boundary conditions on plates*, *J. Phys. A* **35** (2002) 1297–1320, [[hep-th/0007242](#)].
  - [11] G. Aleixo and H. F. S. Mota, *Thermal Casimir effect for the scalar field in flat spacetime under a helix boundary condition*, *Phys. Rev. D* **104** (2021), no. 4 045012, [[arXiv:2105.0822](#)].
  - [12] C. A. Escobar, A. Martín-Ruiz, R. Linares, and J. M. Silva, *A coherent state approach to the Casimir effect for a massive scalar field in a noncommutative spacetime*, *Annals Phys.* **460** (2024) 169570.
  - [13] M. Bordag, G. L. Klimchitskaya, U. Mohideen, and V. M. Mostepanenko, *Advances in the Casimir effect*, vol. 145. OUP Oxford, 2009.
  - [14] K. A. Milton, *The Casimir effect: physical manifestations of zero-point energy*. World Scientific, 2001.
  - [15] V. Mostepanenko, N. Trunov, and R. Znajek, *The Casimir Effect and Its Applications*. Oxford science publications. Clarendon Press, 1997.
  - [16] V. A. Kostelecký and S. Samuel, *Spontaneous breaking of lorentz symmetry in string theory*, *Physical Review D* **39** (1989), no. 2 683.
  - [17] D. Colladay and V. A. Kostelecký, *CPT violation and the standard model*, *Phys. Rev. D* **55** (Jun, 1997) 6760–6774.
  - [18] A. J. D. Farias Junior and H. F. Mota Santana, *Loop correction to the scalar Casimir energy density and generation of topological mass due to a helix boundary condition in a scenario with Lorentz violation*, *Int. J. Mod. Phys. D* **31** (2022), no. 16 2250126, [[arXiv:2204.0940](#)].
  - [19] M. Cruz, E. Bezerra de Mello, and A. Petrov, *Thermal corrections to the casimir energy in a lorentz-breaking scalar field theory*, *Modern Physics Letters A* **33** (05, 2018) 37.
  - [20] A. F. Santos and F. C. Khanna, *Corrections Due to Lorentz Violation, Finite Temperature, and Magnetic Field for the Casimir Effect of a Massive Scalar Field*, *Int. J. Theor. Phys.* **61** (2022), no. 4 96.
  - [21] R. A. Dantas, H. F. S. Mota, and E. R. Bezerra de Mello, *Bosonic casimir effect in an aether-like lorentz-violating scenario with higher order derivatives*, *Universe* **9** (2023), no. 5 241.
  - [22] D. Colladay and V. A. Kostelecký, *Lorentz-violating extension of the standard model*, *Phys. Rev. D* **58** (Oct, 1998) 116002.
  - [23] A. Anisimov, T. Banks, M. Dine, and M. Graesser, *Comments on noncommutative phenomenology*, *Phys. Rev. D* **65** (2002) 085032, [[hep-ph/0106356](#)].

- [24] C. E. Carlson, C. D. Carone, and R. F. Lebed, *Bounding noncommutative qcd*, *Physics Letters B* **518** (2001), no. 1-2 201–206.
- [25] J. L. Hewett, F. J. Petriello, and T. G. Rizzo, *Signals for noncommutative interactions at linear colliders*, *Physical Review D* **64** (2001), no. 7 075012.
- [26] O. Bertolami and L. Guisado, *Noncommutative field theory and violation of translation invariance*, *Journal of High Energy Physics* **2003** (2003), no. 12 013.
- [27] V. A. Kostelecký, R. Lehnert, and M. J. Perry, *Spacetime-varying couplings and lorentz violation*, *Physical Review D* **68** (2003), no. 12 123511.
- [28] L. Anchordoqui and H. Goldberg, *Time variation of the fine structure constant driven by quintessence*, *Physical Review D* **68** (2003), no. 8 083513.
- [29] O. Bertolami, *Lorentz invariance and the cosmological constant*, *Classical and Quantum Gravity* **14** (1997), no. 10 2785.
- [30] J. Alfaro, H. A. Morales-Tecotl, and L. F. Urrutia, *Quantum gravity corrections to neutrino propagation*, *Physical Review Letters* **84** (2000), no. 11 2318.
- [31] J. Alfaro, H. A. Morales-Tecotl, and L. F. Urrutia, *Loop quantum gravity and light propagation*, *Physical Review D* **65** (2002), no. 10 103509.
- [32] P. Hořava, *Quantum gravity at a lifshitz point*, *Physical Review D* **79** (2009), no. 8 084008.
- [33] I. M. Ulion, E. B. de Mello, and A. Yu. Petrov, *Casimir effect in horava-lifshitz-like theories*, *International Journal of Modern Physics A* **30** (2015), no. 36 1550220.
- [34] R. Jackiw, *Functional evaluation of the effective potential*, *Phys. Rev. D* **9** (1974) 1686.
- [35] D. Anselmi, *Weighted power counting and lorentz violating gauge theories. i: General properties*, *Annals of Physics* **324** (2009), no. 4 874–896.
- [36] D. Anselmi, *Weighted power counting and lorentz violating gauge theories. ii: Classification*, *Annals of Physics* **324** (2009), no. 5 1058–1077.
- [37] L. H. Ryder, *Quantum field theory*. Cambridge university press, 1996.
- [38] D. J. Toms, *Symmetry Breaking and Mass Generation by Space-time Topology*, *Phys. Rev. D* **21** (1980) 2805.
- [39] M. B. Cruz, E. R. Bezerra de Mello, and H. F. Santana Mota, *Casimir energy and topological mass for a massive scalar field with Lorentz violation*, *Phys. Rev. D* **102** (2020), no. 4 045006, [[arXiv:2005.0951](https://arxiv.org/abs/2005.0951)].
- [40] P. J. Porfírio, H. F. Santana Mota, and G. Q. Garcia, *Ground state energy and topological mass in spacetimes with nontrivial topology*, *Int. J. Mod. Phys. D* **30** (2021), no. 08 2150056, [[arXiv:1908.0051](https://arxiv.org/abs/1908.0051)].
- [41] A. J. D. F. Junior and H. F. S. Mota, *Casimir effect, loop corrections, and topological mass generation for interacting real and complex scalar fields in minkowski spacetime with different conditions*, *Phys. Rev. D* **107** (Jun, 2023) 125019.
- [42] S. W. Hawking, *Zeta Function Regularization of Path Integrals in Curved Space-Time*, *Commun. Math. Phys.* **55** (1977) 133.
- [43] I. S. Gradshteyn and I. M. Ryzhik, *Table of integrals, series, and products*. Academic press, 2014.
- [44] L. H. Ford, *Vacuum polarization in a nonsimply connected spacetime*, *Phys. Rev. D* **21** (Feb, 1980) 933–948.
- [45] A. A. Saharian, *The generalized abel-plana formula with applications to bessel functions and casimir effect*, 2007.
- [46] M. Abramowitz and I. A. Stegun, *Handbook of mathematical functions dover publications*, New York **361** (1965).
- [47] M. B. Cruz, E. R. B. de Mello, and A. Y. Petrov, *Casimir effects in lorentz-violating scalar field theory*, *Phys. Rev. D* **96** (Aug, 2017) 045019.
- [48] M. Bordag, U. Mohideen, and V. M. Mostepanenko, *New developments in the casimir effect*, *Physics reports* **353** (2001), no. 1-3 1–205.
- [49] G. B. Arfken, H. J. Weber, and F. E. Harris, *Mathematical methods for physicists: a comprehensive guide*. Academic press, 2011.
- [50] D. J. Toms, *Interacting Twisted and Untwisted Scalar Fields in a Nonsimply Connected Space-time*, *Annals Phys.* **129** (1980) 334.
- [51] F. Pascoal, L. Oliveira, F. Rosa, and C. Farina, *Estimate for the size of the compactification radius of a one extra dimension universe*, *Brazilian Journal of Physics* **38** (2008) 581–586.